Protein Engineering vol.11 no.10 pp.873–879, 1998

Concerted motions in the photoactive yellow protein

D.M.F. van Aalten[1], W.D.Hoff[2], J.B.C.Findlay, W.Crielaard[2] and K.J.Hellingwerf[2]

Department of Biochemistry and Molecular Biology, University of Leeds, Leeds LS2 9JT, UK and [2]Department of Microbiology, E.C. Slater Institute, BioCentrum University of Amsterdam, The Netherlands

[1]To whom correspondence should be addressed at present address: Keck Structural Biology, Cold Spring Harbor Laboratory, 1 Bungtown Road, Cold Spring Harbor, NY 11724, USA

Molecular dynamics simulations have been performed with the aim of identifying concerted backbone motions in the photoactive yellow protein. Application of the essential dynamics method revealed large, chromophore-linked fluctuations of the protein in the ground state, as well as in a form containing the isomerized chromophore. Various loops become more mobile upon isomerization of the chromophore, including a loop which is part of the PAS domain motif, found in light perception proteins. The hinge points identified in these fluctuations correlate with the positions of evolutionary conserved glycines. The results derived from the simulations directly correlate with available experimental data, provide a framework for understanding the dynamic behaviour of the yellow protein and give clues to subsequent steps in the signal transduction pathway.

Keywords: chromophore/essential dynamics/molecular dynamics/photocycle/photo-active yellow protein/*p*-coumaric acid

Introduction

The photoactive yellow protein (PYP) is a member of the xanthopins (Kort *et al.*, 1996a), a family of water-soluble photoreceptors of which the first representative was isolated from *Ectothiorhodospira halophila*. This bacterium can be found in saline, sun-bathed lakes (e.g. Wadi Natrun in Egypt; Imhoff *et al.*, 1978; Meyer, 1985, 1987). The protein is thought to be involved in phototactic responses of the bacterium to blue light (Sprenger *et al.*, 1993). It binds a recently identified chromophore, *p*-coumaric acid (which gives the protein its characteristic yellow colour), via a thio-ester linkage to a unique cysteine (Hoff *et al.*, 1994a, Baca *et al.*, 1994). Initial attempts to solve the structure of the protein resulted in the proposal of a β-clam structure (McRee *et al.*, 1986, 1989). Recent efforts, however, have culminated in a 1.4 Å resolution structure for the ground state of PYP and its chromophore (Baca *et al.*, 1994; Borgstahl *et al.*, 1995) (see Figure 1). This structure reveals an α/β fold, with the chromophore buried in its charged state (i.e. deprotonated, as indicated by spectral studies (Kim *et al.*, 1995; Hoff *et al.*, 1996) in a pocket, tethered by several hydrogen bonds. The PYP photocycle consists of three states, the ground state (pG) with a UV/VIS absorbance maximum of 446 nm, a red-shifted intermediate (pR), absorbing at 465 nm [formed on a ps time scale (Baltuska *et al.*, 1997; Changenet *et al.*, 1997), presumably involving a double bond isomerization in *p*-coumaric acid (Kort *et al.*, 1996b)], which converts on the ms time scale to a second, transient blue-shifted intermediate (pB), absorbing at 355 nm. The pB intermediate subsequently relaxes back to pG on a sub-second time scale (Meyer *et al.*, 1987, 1991; Hoff *et al.*, 1992, 1994b). Although the crystal structure of PYP enhances our knowledge of pG, it does not provide any clues to the events that take place during the PYP photocycle. However, various other biophysical studies, summarized below, have been directed towards resolving a number of physical properties of PYP which change during the photocycle.

- The fact that the absorbance spectrum of PYP changes during the photocycle indicates that the environment of the chromophore changes.
- The suggestion that PYP is involved in the phototactic response of *E.halophila* implies that there is a light triggered (not necessarily direct) interaction between the protein and the flagellar machinery; i.e. a signalling state must be formed.
- A hydrophobic patch is exposed to the solvent during the lifetime of pB (Meyer *et al.*, 1989; Salamon *et al.*, 1995; van Brederode *et al.*, 1996).
- Changes in the volume of PYP occur upon formation of pR (van Brederode *et al.*, 1995).
- The photocycle induces the uptake and subsequent release of a single proton (Meyer *et al.*, 1993). This may be attributed to protonation/deprotonation of the chromophore (Baca *et al.*, 1994; Kim *et al.*, 1995; Hoff *et al.*, 1996).
- Thermodynamic analysis of the temperature dependence of the PYP photocycle kinetics has shown that PYP partially unfolds upon formation of pB (Hoff *et al.*, 1995; van Brederode *et al.*, 1996).
- Laue crystallography has indicated that the chromophore is transiently exposed to the solvent (Genick *et al.*, 1997).

To correlate this wealth of biophysical data with the available high-resolution crystal structure of PYP, we have produced molecular dynamics (MD) simulations of PYP, prior and subsequent to isomerization of the chromophore, with the aim of investigating the differences in conformational freedom of these two forms of the yellow protein.

Methods

Calculations were started from the high resolution PYP X-ray structure (Borgstahl *et al.*, 1995) [entry 2PHY in the Brookhaven Protein Databank (Bernstein *et al.*, 1977)] using the GROMOS suite of programs (van Gunsteren and Berendsen, 1987). The protein (125 residues) was solvated in a truncated octahedral box filled with SPC (Berendsen *et al.*, 1981) water molecules. The net charge of –6.0 was compensated for by replacing water molecules at the six most electrostatically negative positions with sodium ions. This resulted in a system with 10 292 atoms. Twenty-five steps of steepest descents minimization were performed to relax possible strain in the molecule. A pair list cut-off of 8 Å was used, together with a 10 Å long-range electrostatic cut-off. Velocities were then generated by taking them from a Maxwellian distribution

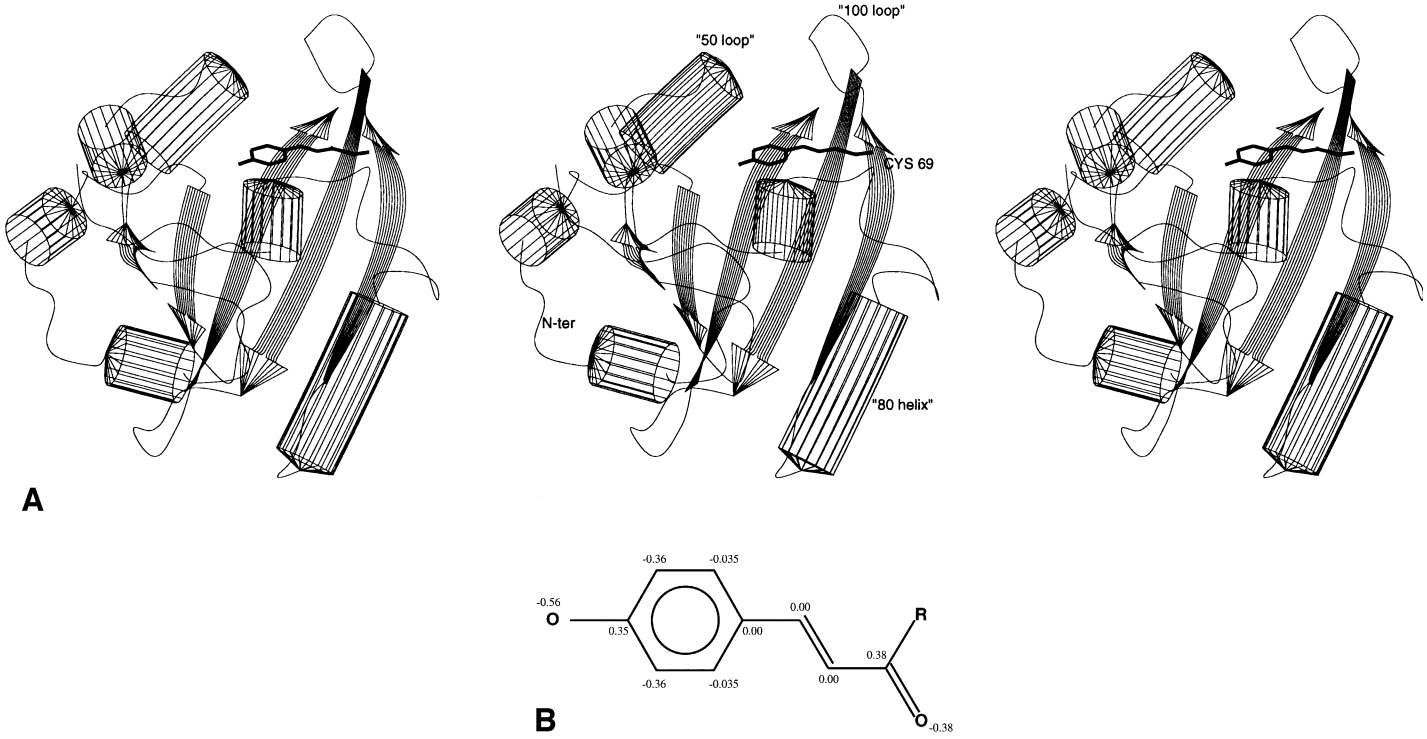

Fig. 1. (**A**) Stereo picture of the PYP crystal structure (Borgstahl *et al.*, 1995) defining certain regions in the protein which will be referred to in the text. (**B**) Picture of the PYP chromophore, *p*-coumaric acid. Atomic charges used in the simulations are given.

at 300 K. The simulation was continued for 550 ps using temperature (τ_T = 0.1 ps) and pressure (τ_p = 0.5 ps) coupling (Berendsen *et al.*, 1984). Application of the SHAKE algorithm to constrain bond lengths (Ryckaert *et al.*, 1977) allowed a time step of 2 fs. Coordinate trajectory frames were stored at a rate of 20 per ps.

The simulation of the yellow protein with isomerized chromophore (from now on called PYP#) was started from the 200 ps structure of the PYP simulation (isomerization of the chromophore was achieved by temporarily removing the double bond potential) and continued for 450 ps. The last 400 ps of both simulations were used for essential dynamics analyses.

Essential dynamics (Amadei *et al.*, 1993) is based on the diagonalization of the covariance matrix built from atomic fluctuations in an MD trajectory:

$$C_{ij} = < (x_i - x_{i,0}) (x_j - x_{j,0}) > \quad (1)$$

where $x_{i,j}$ are separate *x,y,z* coordinates of the atoms, x_0 the average positions of the coordinates and the average is calculated over the whole trajectory. Diagonalization yields a set of eigenvectors and eigenvalues, which are sorted by size of the eigenvalue (i.e. the 'first' eigenvector is the eigenvector with the largest eigenvalue). The eigenvectors indicate directions in the 3*N configurational space, representing correlated displacements of groups of atoms in the protein. The corresponding eigenvalues indicate the amplitude of these correlated motions. It has been shown that essential dynamics is a useful technique for revealing functionally significant fluctuations in various proteins, such as lysozyme (Amadei *et al.*, 1993), thermolysin (van Aalten *et al.*, 1995a), the SH3 signalling domain (van Aalten *et al.*, 1996a) and the cellular retinol binding protein (van Aalten *et al.*, 1995b).

A useful enhancement of the essential dynamics technique is the so-called 'combined analysis' (van Aalten *et al.*, 1995a). MD trajectories of similar systems are concatenated to form one big trajectory, from which the covariance matrix is built and eigenvectors extracted. These eigenvectors now indicate directions (concerted fluctuations of atoms) which are *common* in the separate trajectories. Dynamic differences in the separate trajectories can be investigated by projecting them onto the common eigenvectors. The mean square fluctuation in the projection indicates the dynamic behaviour (amplitude of the fluctuation) of the system along the direction described by the eigenvector. Here, we combine the PYP and PYP# trajectories to analyse differences in dynamics using this 'combined analysis' technique.

Hinges in the protein were detected using the moving window r.m.s.d. method recently described elsewhere (van Aalten *et al.*, 1995b). In short, this involves superposing Cα atoms of sequential peptides from two conformations of a protein. If the conformations of the region represented by the peptides are similar, a low root mean square deviation (r.m.s.d.) will be obtained. A large r.m.s.d. is obtained when there are some variations in backbone ϕ/ψ torsion angles, thus detecting the possible presence of a hinge residue. Here, we superimpose the two most structurally distant structures found in the eigenvector motions of PYP, to identify hinge residues which are important for producing these motions.

The small molecule topology for *p*-coumaric acid was generated from the coordinates of the chromophore in the PYP crystal structure using PRODRG (which uses standard GROMOS forcefield parameters) (van Aalten *et al.*, 1996b) and attached to a standard GROMOS cysteine topology. Partial atomic charges (see Figure 1B) were modelled on the standard collection of GROMOS topology building blocks and remained static throughout the simulation. Hence a detailed study of the photo-isomerization is not possible within the framework of this

investigation, the *cis* and *trans* forms were studied separately. Simulation structures were analysed using WHAT IF (Vriend, 1990). Various structural properties were calculated using DSSP (Kabsch and Sander, 1983). Simulations were performed on the Cray YMP of the SARA Computer Centre, Amsterdam.

Results

Stability of the simulation

Before the trajectories can be used for essential dynamics analyses, it is necessary to examine their stability. Several structural properties (r.m.s.d. with respect to the starting structure, hydrogen bonds, solvent accessibility) were calculated as a function of simulation time (Figure 2). These properties appeared to be stable for both simulations, although a small drift is observed in the r.m.s.d. for the PYP# simulation. This does, however, not represent unfolding of the protein, as the other geometrical properties are stable. Below, we analyze this motion in terms of large, concerted backbone fluctuations.

Recently, it was reported that there is a change in PYP volume during entry into its photocycle (van Brederode *et al.*, 1995). The radius of gyration, a property linked to the volume, was compared for PYP and PYP#. On average, PYP# (13.19 Å) is slightly smaller than PYP (13.23 Å), which is in agreement with the experimental results. As will be shown below, this volumetric change is reflected in the large atomic motions as revealed by essential dynamics.

Visual inspection

Visual inspection of the PYP# trajectory revealed that within 50 ps of equilibration, the *cis*-chromophore had changed position in the binding pocket, pointing upwards with its hydroxyl group towards the solvent (Figure 3). The loops around residues 50 and 100 (see also Figure 1) had changed conformation. Arg52, Thr50 and Glu46, all involved in binding the chromophore in PYP had lost most of their interaction with the chromophore. Since the chromophore is now bent away from Glu46, pointing towards the solvent, it is likely to be a candidate for protonation. This correlates with the observation that the chromophore may become protonated during the initial stages of the photocycle (Meyer *et al.*, 1993; Baca *et al.*, 1994; Hoff *et al.*, 1994a; Kim *et al.*, 1995).

Essential dynamics analysis

Since we have shown that the PYP and PYP# trajectories are stable and that conventional analysis of these trajectories can explain some of the biophysical data available, the concerted motions in PYP can now be examined by the essential dynamics method (Amadei *et al.*, 1993). The PYP and PYP# 400 ps trajectories were concatenated for a 'combined analysis' (see Methods section). A covariance matrix was constructed from the Cα and chromophore atoms only. The Cα atoms have been shown to contain all relevant backbone motions (Amadei *et al.*, 1993; van Aalten *et al.*, 1997). By including the chromophore we can also study correlated motions between the chromophore and the protein backbone. The 408 dimensional matrix [3*(125 Cα + 11 chromophore atoms)] was diagonalized, yielding a set of 'combined' eigenvectors, i.e. eigenvectors which describe identical motions in the PYP and PYP# trajectories. As set out in the Methods section, these combined eigenvectors can be used to study differences in dynamics between the trajectories concatenated. The differences in dynamics can be studied by comparing the mean square fluctuation in these projections (Figure 4). There are significant

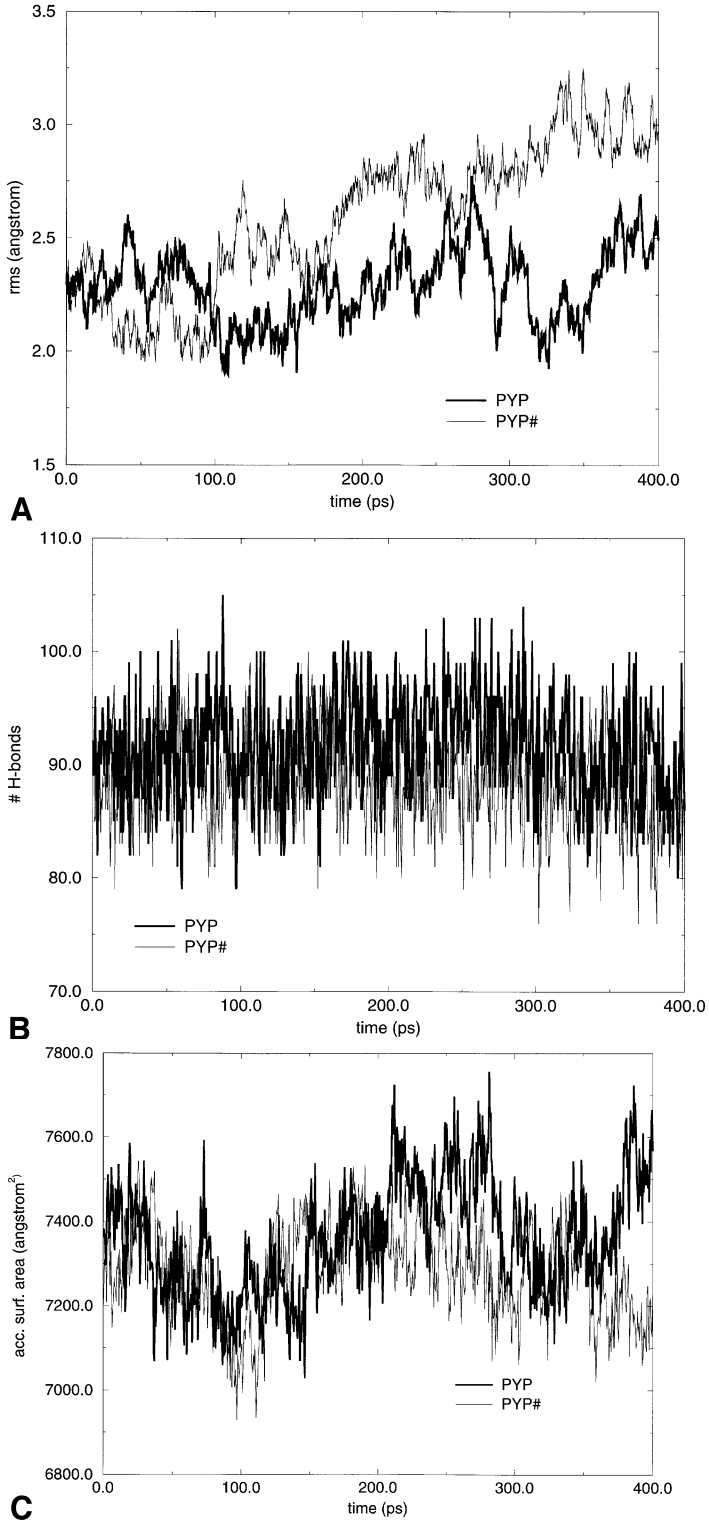

Fig. 2. Analysis of geometrical properties as a function of simulation time. (**A**) R.m.s.d. with respect to the 2PHY X-ray structure. (**B**) Number of backbone hydrogen bonds. (**C**) Total solvent accessible area.

differences in the dynamic behaviour of the two simulations along the combined eigenvectors. The direction described by eigenvector 1 is more accessible for PYP# than for PYP. Similar observations are made for the motions described by eigenvectors 2 and 3, which are rather restricted in PYP but allowed in PYP#. Although restrained when compared with

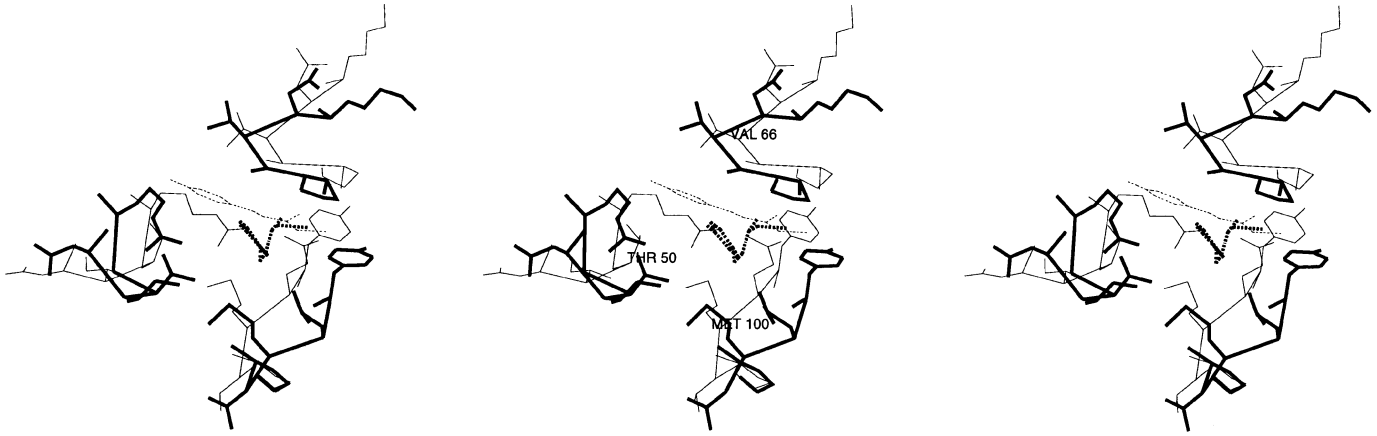

Fig. 3. Stereo picture of the superposition of the chromophore and its pocket in the PYP crystal structure (thin line) and the structure at the end of the PYP# simulation (bold line). The chromophore is depicted using a dotted line. Cα and side chain atoms are depicted using a solid line. Residues 50, 66 and 100 (see also Figure 1) are identified.

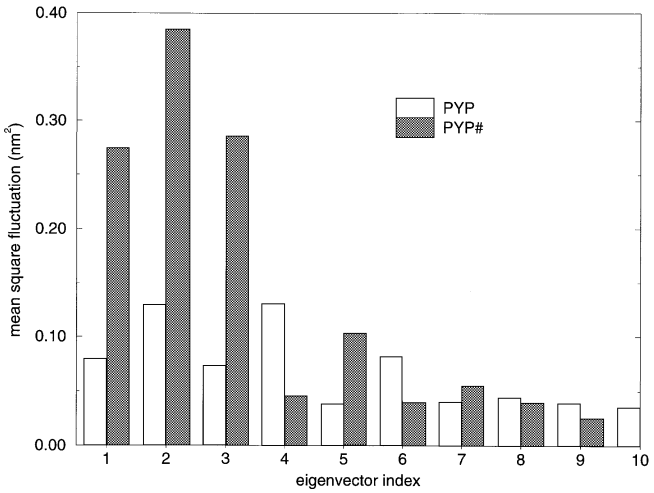

Fig. 4. Analysis of the projection of the separate PYP and PYP# trajectories onto the combined eigenvectors. The mean square fluctuation in these projections reveals differences in dynamic behaviour of the separate PYP and PYP# trajectories in directions described by the combined eigenvectors.

PYP#, these first three eigenvectors are the largest concerted motions in PYP (Figure 4). Thus, conformational freedom, which is already present in PYP, is amplified after isomerization of the chromophore.

The motions described by eigenvectors 1–3 (Figure 5) show common features. Basically, there are two domains in the protein, separated by the rigid β-sheet. The first domain, termed the N-terminal domain, encompasses residues 1–30. The second domain, termed the chromophore domain, is located on the opposite side of the β-sheet. Apart from this β-sheet, the two domains are linked by the highly mobile loop around residue 50. Exchange of the *trans* form with the *cis* form of the chromophore causes it to be pushed out of its pocket. This leads to two effects:

- interactions between the chromophore and residues in the '50-loop' cause this loop (including the helix, see also Figure 1) to follow the motion of the chromophore. This, in turn, leads to fluctuation in the N-terminal domain: the second helix (around residue 20) follows the motion of the '50-loop', which causes a further fluctuation in both the first helix and in the N-terminal residues;
- the mobility of the chromophore is correlated to two motions in the 'chromophore domain'. The '100-loop' moves towards the chromophore and the '80-helix' is compressed along its main axis.

Recently we have used the moving window r.m.s.d. method (see Methods) to identify hinge bending regions in the cellular retinol binding protein (van Aalten *et al.*, 1995b). A few highly conserved glycines were identified at the centre of these regions. The results from this method as applied to the structures from the combined eigenvectors are shown in Figure 6. It appears that there are a few localized hinge bending regions which are active in the eigenvector motions. The peaks close to residues 7, 50, 75 and 90 (and possibly 110) indicate hinges which are present in all three eigenvector motions. The hinge bending near residue 25, however, seems to occur mainly in eigenvector 1. When these hinge locations are compared with a PYP sequence alignment (Figure 7), it appears that there are conserved glycines in or near the areas identified by the peaks in Figure 6 (Gly7, Gly29, Gly47, Gly77 and Gly86). These conserved, flexible glycines seem to play an important role in the mechanics of the protein, as observed for other proteins previously (van Aalten *et al.*, 1995a,b).

Discussion and conclusion

The chromophore

Our simulations reveal the crucial role of the chromophore in structure and dynamics of PYP. The chromophore lies in a pocket which is connected to other areas in the protein via several loops. Essential dynamics analysis of the simulations reveal amplification of the large concerted motions upon exchange of the *trans* with the *cis* form of the chromophore. This implies that the *trans* form of the chromophore may prevent the protein from undergoing a conformational change. Upon chromophore isomerization (and subsequent displacement of the chromophore) several large concerted fluctuations were enhanced. This will ultimately have to lead to a signal, influencing the swimming pattern of the bacterium.

The protein

The two 400 ps PYP simulations described here are reliable as estimated from several geometrical properties. Although the PYP# simulation seems to show a continuous drift away from the X-ray structure, there is a biological explanation for

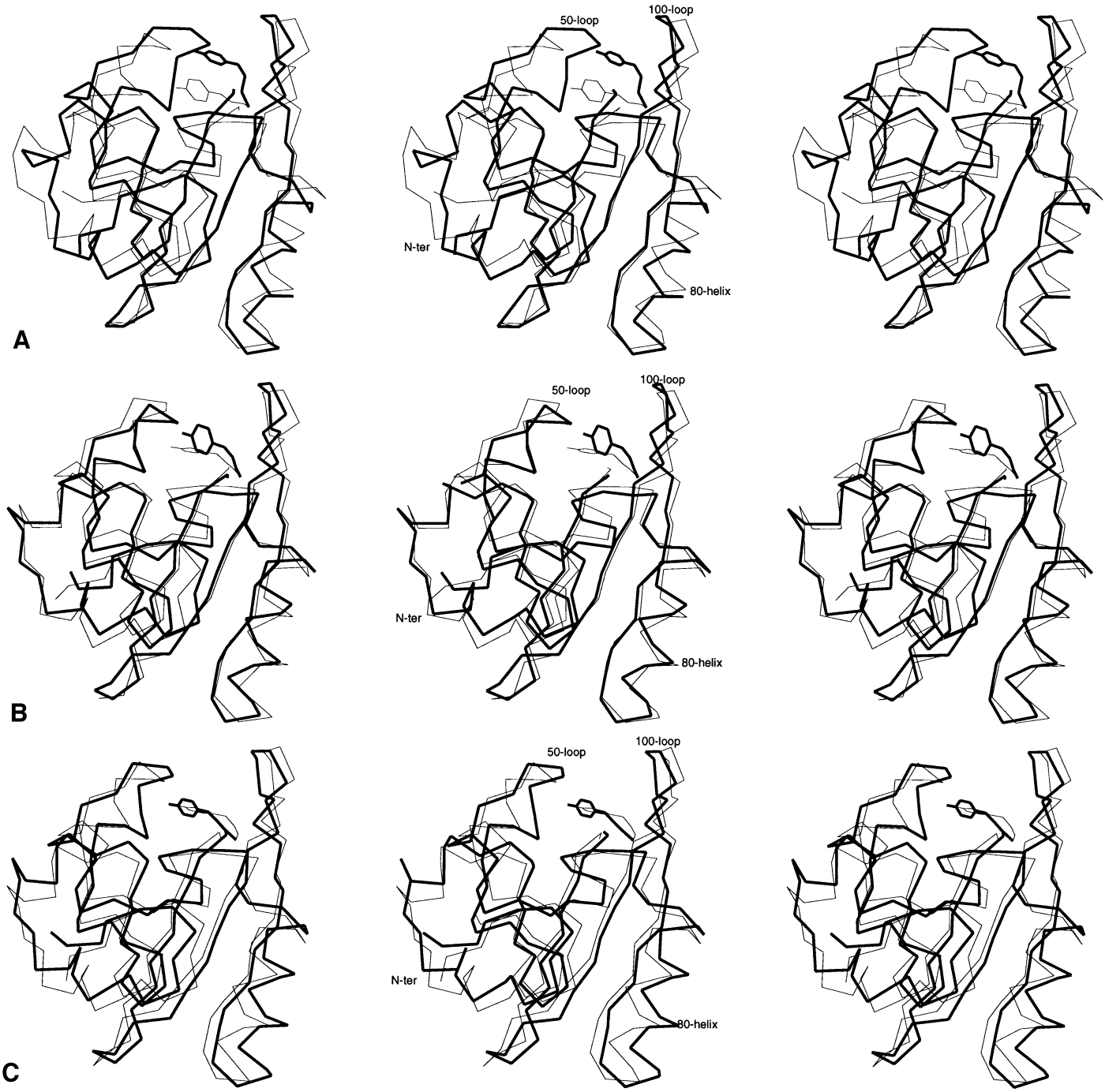

Fig. 5. Representation of the motions found in the first three eigenvectors of the combined analysis (stereo pictures). For each eigenvector (1 = A, 2 = B, 3 = C), the MD structures with the minimum (bold line) and the maximum projection (thin line) are shown. (Differences in dynamic behaviour along these eigenvectors are indicated in Figure 4). The N-terminal domain, the 50 and 100 loops and the 80 helix are identified.

this. After bleaching, pB is formed (via pR) on a sub-ms time scale. Clearly, an MD simulation on a ps time scale cannot properly determine the final structure of pB. Together with essential dynamics, however, these simulations can be used to identify the direction of drifts in the structure and these may represent a drift towards the structure of pB.

Conventional examination of the trajectories revealed several features which could be linked to biophysical data for PYP, such as the protonation state of the chromophore and the volume of the protein. This correlation with available experimental data confirms the idea that the simulations were stable and reliable.

The main aim of our study was to detect chromophore-linked fluctuations in the protein. The essential dynamics technique, applied to the PYP and PYP# trajectories enabled us to do this. Interestingly, the analysis showed that the *type* of concerted motions found in PYP and PYP# were similar. This indicates that there is already a fluctuation, in the direction of PYP#, in PYP. This supports the hypothesis that the *trans* form of chromophore inhibits fluctuations/conformational change. Isomerization of the chromophore allows much larger fluctuations along the essential eigenvectors, which may ultimately lead to a structural transition. So, although the *type* of

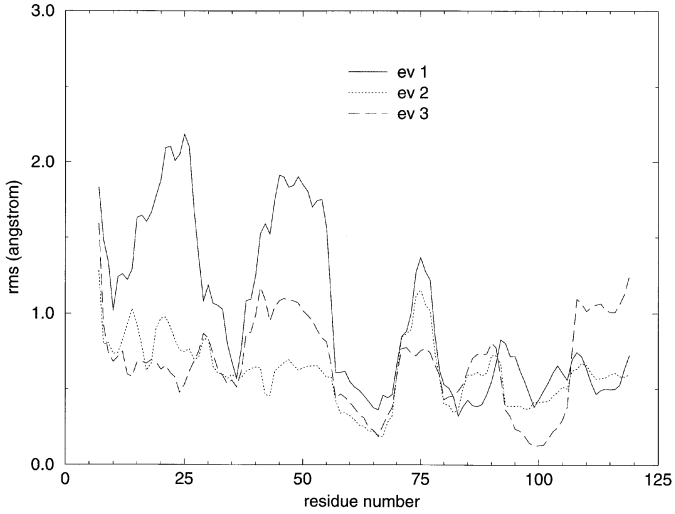

Fig. 6. Results from the moving window r.m.s.d. method (see Methods). Peaks identify hinge residues. For each eigenvector the MD structures with the minimum and maximum projections (i.e. the structures which are conformationally the most distant along that eigenvector) were used.

concerted motions found in PYP and PYP# are similar, the amplitude of the fluctuations of PYP and PYP# along these motions differs. The first three eigenvectors are all significantly more accessible in PYP# than in PYP.

The eigenvector motions provide a detailed description of the mechanical construction of the protein. We have demonstrated that the motion of the chromophore is translated into motions of several backbone segments, joined together by flexible hinges, which are mostly conserved glycines. The amounts of fluctuation and conformational change point to the two most likely candidates for a signaling domain which transmits the light signal to the next component in the signal-transduction chain that is initiated by PYP. One of these is the '50-loop', which fluctuates over a considerable distance, linked to the chromophore. Interestingly, this loop is part of the PAS domain, a sequence motif found in a range of protein involved in light perception and clock proteins (Crosthwaite *et al.*, 1997). Gly47 and Gly51, which might be involved in hinge bending in PYP (Figures 6 and 7), are part of the PAS domain motif. Another candidate for signal transduction is the N-terminal domain, which is somewhat separate from the rest of the protein and is linked to the chromophore via the '50-loop'. Interestingly, a PYP sequence alignment (Figure 7) shows that this N-terminal domain is highly variable. This may point to interaction with different proteins among the various PYP homologues.

In short, the simulations have increased our insight in PYP structure and function. On the basis of the interpretations given above, several mutations can be proposed, influencing the interaction of PYP with the chromophore, the transition of the chromophore isomerization signal to the rest of the protein and the interaction with a possible signal transducer.

References

Amadei,A., Linssen,A.B.M. and Berendsen,H.J.C. (1993) *Proteins*, **17**, 412–425.

Baca,M., Borgstahl,G.E.O., Boissinot,M., Burke,P.M., Williams,D.R., Slater,K.A. and Getzoff,E.D. (1994) *Biochemistry*, **33**, 14369–14377.

Baltuska,A., van Stokkum,I.H.M., Kroon,A., Monshouwer,R., Hellingwerf,K.J. and van Grondelle,R. (1997) *Chem. Phys. Lett.*, **270**, 263–266.

Berendsen,H.J.C., Postma,J.P.M., DiNola,A. and Haak,J.R. (1984) *J. Chem. Phys.*, **81**, 3684–3690.

Berendsen,H.J.C., Postma,J.P.M., van Gunsteren,W.F. and Hermans,J. (1981) In Pullmann,B. (ed.), *Intermolecular Forces*. Reidel, Dordrecht, p. 331.

Bernstein,F.C., Koetzle,T.F., Williams,G.J.B., Meyer,E.F., Brice,M.D., Rodgers,J.R., Kennard,O., Shimanouchi,T. and Tasumi,M. (1977) *J. Mol. Biol.*, 1**12**, 535–542.

Borgstahl,G.E.O., Williams,D.R. and Getzoff,E.D. (1995) *Biochemistry*, **34**, 6278–6287.

Changenet,P., Zhang,H., van der Meer,M., Hellingwerf,K.J. and Glasbeek,M. (1998) *Phys. Chem. Lett.*, in press.

Crosthwaite,S.K., Dunlap,J.C. and Loros,J.J. (1997) *Science*, **276**, 763–769.

Genick,U.K., Borgstahl,G.E.O., Kingman,N., Ren,Z., Pradervand,C., Burke,P., Srajer,V., Teng,T., Schildkamp,W., McRee,D.E., Moffat,K. and Getzoff,E.D. (1997) *Science*, **275**, 1471–1475.

Hoff,W.D., Kwa,S.L.S., van Grondelle,R. and Hellingwerf,K.J. (1992) *Photochem. Photobiol.*, **56**, 529–539.

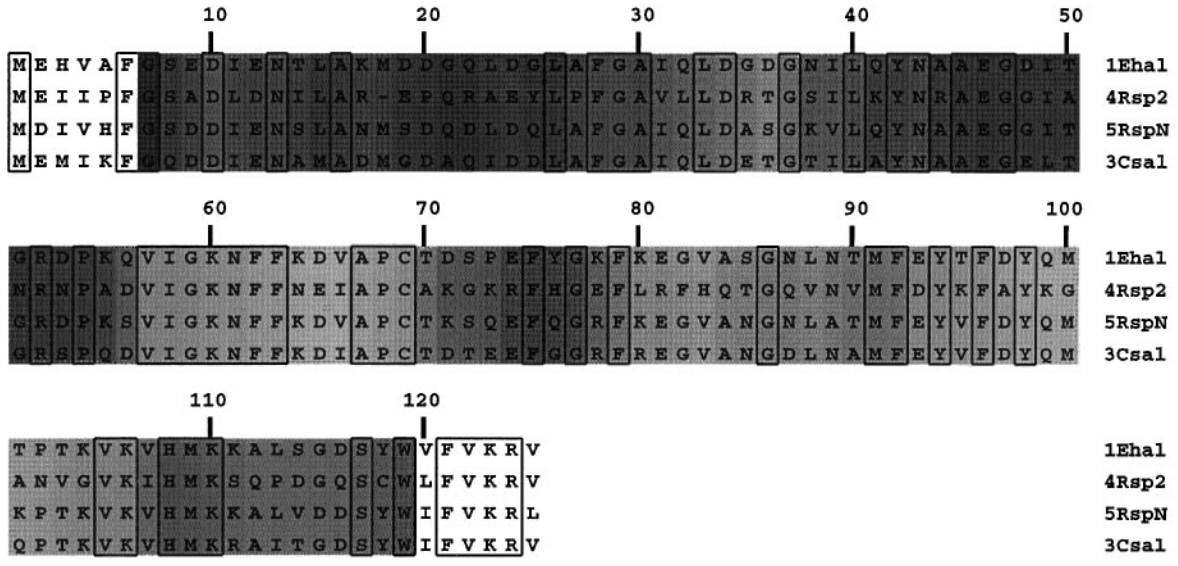

Fig. 7. Sequence alignment of PYP isolated from various species. 1Ehal = *E.halophila*, 4rsp2 = *Rhodobacter spaeroides*, 3Csal = *Chromatium salexigens*, 2Rsal = *Rhodospirillum salexigens*. Boxes indicate conserved residues. Grey scale indicates hinge bending residues (see Figure 5). White, no hinge bending; dark grey, highest peak in Figure 5.

Hoff,W.D., Düx,P., Devreese,B., Nugteren-Roodzant,I.M., Crielaard,W., Boelens,R., Kaptein,R., van Beeumen,J. and Hellingwerf,K.J. (1994a) *Biochemistry*, **33**, 13959–13962.
Hoff,W.D., van Stokkum,I.H.M., van Ramesdonk,H.J., van Brederode,M.E., Brouwer,A.M., Fitch,J.C., Meyer,T.E., van Grondelle,R. and Hellingwerf,K.J. (1994b) *Biophys. J.*, **67**, 1691–1705.
Hoff,W.D., Matthijs,H.C.P., Schubert,H., Crielaard,W. and Hellingwerf,K.J. (1995) *Biophys. Chem.*, **56**, 193–199.
Hoff,W.D., Devreese,B., Fokkens,R., Nugteren-Roodzant,I.M., van Beeumen,J.F., Nibbering,N. and Hellingwerf,K.J. (1996) *Biochemistry*, **35**, 1274–1281.
Imhoff,J.F., Hashwa,F. and Trüper,H.G. (1978) *Arch. Hydrobiol.*, **84**, 381–388.
Kabsch,W. and Sander,C. (1983) *Biopolymers*, **22**, 2577–2637.
Kim,M., Mathies,R.A., Hoff,W.D. and Hellingwerf,K.J. (1995) *Biochemistry*, **34**, 12669–12672.
Kort,R., Hoff,W.D., van West,M., Kroon,A.R., Hoffer,S.M., Vlieg,K.H., Crielaard,W., van Beeumen,J.J. and Hellingwerf,K.J. (1996a) *EMBO J.*, **15**, 3209–3218.
Kort,R., Vonk,H., Xu,X., Hoff,W.D., Crielaard,W. and Hellingwerf,K.J. (1996b) *FEBS Lett.*, **32**, 73–78.
McRee,D.E., Meyer,T.E., Cusanovich,M., Parge,H.E. and Getzoff,E.D. (1986) *J. Biol. Chem.*, **261**, 13850–13851.
McRee,D.E., Tainer,J.A., Meyer,T.E., van Beeumen,J., Cusanovich,M.A. and Getzoff,E.D. (1989) *Proc. Natl Acad. Sci. USA*, **86**, 6533–6537.
Meyer,T.E. (1985) *Biochim. Biophys. Acta*, **806**, 175–183.
Meyer,T.E., Yakali,E., Cusanovich,M.A. and Tollin,G. (1987) *Biochemistry*, **26**, 418–423.
Meyer,T.E., Tollin,G., Hazzard,J.H. and Cusanovich,M.A. (1989) *Biophys. J.*, **56**, 559–564.
Meyer,T.E., Tollin,G., Causgrove,T.P., Cheng,P. and Blankenship,R.E. (1991) *Biophys. J.*, **59**, 988–991.
Meyer,T.E., Cusanovich,M.A. and Tollin,G. (1993) *Arch. Biochem. Biophys.*, **306**, 515–517.
Ryckaert,J.P., Ciccotti,G. and Berendsen,H.J.C. (1977) *J. Comp. Phys.*, **23**, 327–341.
Salamon,Z., Meyer,T.E. and Tollin,G. (1995) *Biophys. J.*, **68**, 648–654.
Sprenger,W.W., Hoff,W.D., Armitage,J.P. and Hellingwerf,K.J. (1993) *J. Bacteriol.*, **175**, 3096–3104.
van Aalten,D.M.F., Amadei,A., Linssen,A.B.M., Eijsink,V.G.H., Vriend,G. and Berendsen,H.J.C. (1995a) *Proteins*, **22**, 45–54.
van Aalten,D.M.F., Findlay,J.B.C., Amadei,A. and Berendsen,H.J.C. (1995b) *Prot. Engng*, **8**, 1129–1135.
van Aalten,D.M.F., Amadei,A., Bywater,R., Findlay,J.B.C., Berendsen,H.J.C., Sander,C. and Stouten,P.F.W. (1996a) *Biophys. J.*, **70**, 684–692.
van Aalten,D.M.F., Bywater,R., Findlay,J.B.C., Hendlich,M., Hooft,R.W.W. and Vriend,G. (1996b) *JCAMD*, **10**, 255–262.
van Aalten,D.M.F., de Groot,B.L., Findlay,J.B.C., Berendsen,H.J.C. and Amadei,A. (1997) *J. Comp. Chem.*, **18**, 169–181.
van Brederode,M.E., Gensch,T., Hoff,W.D., Hellingwerf,K.J. and Braslavsky,S.E. (1995) *Biophys.J.*, **68**, 1101–1109.
van Brederode,M.E., Hoff,W.D., van Stokkum,I.H.M., Groot,M.L. and Hellingwerf,K.J. (1996) *Biophys. J.*, **71**, 365–380.
van Gunsteren,W.F. and Berendsen,H.J.C. (1987) *Gromos Manual*. BIOMOS, Biomolecular Software, Laboratory of Physical Chemistry, University of Groningen, The Netherlands.
Vriend,G. (1990) *J. Mol. Graph.*, **8**, 52–56.

Received April 15, 1997; revised February 5, 1998; accepted June 1, 1998